ELSEVIER

Human Movement Science 15 (1996) 477–496

HUMAN MOVEMENT SCIENCE

Biomechanics of the upper limb using robotic techniques

L. Chèze, C. Gutierrez *, R. San Marcelino, J. Dimnet

Laboratory of Motion Biomechanics, University of Lyon I, Bâtiment 721, 43 Bd du 11 novembre 1918, 69622 Villeurbanne Cedex, France

Abstract

Motion biomechanics in living subjects is very often obtained from data provided by optoelectronic systems. They describe 3-dimensional trajectories of either emitting or reflective markers fixed upon subject body segments. Is it possible to use these trajectories to define the 3-dimensional kinematics of articular groups while carrying out a task? In this paper, the methodology to determine the movements of the internal structure of an upper limb from external marker trajectories is described. Each body segment (trunk, arm, forearm, hand) is labeled by reflective markers. The individual trajectories are numerically treated so that each segment can be considered as a solid for which laws of solid mechanics can be applied. A mechanism is introduced to represent the functional anatomy of the upper limb carrying out a task. The laws of displacements of this mechanism restitute the motion of body segments known from the external markers trajectories. The structure of the mechanism is defined from pretestings to determine the flexion and rotation axes of body segments, the centers of rotation and their corresponding scattering. A robotic approach is used so as to numerically describe the upper limb whilst carrying out a task. The mechanical structure is a complex structure of longitudinal links representing human body segments. These links are connected together by the mean of articular groups. Each of these groups have 3 angular degrees of freedom (df). Experimental testings have been performed using anatomic specimens of the upper limb. They focus upon geometrical constraints existing between the 3 angular df of each articular group. The corresponding laws of motion obtained on cadavers are assumed to be representative of the bony structure of living subjects. The

* Corresponding author. E-mail: corinne@biomeca.univ-lyonl.fr. Tel.: +33 72 448573. Fax: +33 72 448054.

0167-9457/96/$15.00
PII S0167-9457(96)00011-5

structure of the mechanism is then modified to take into account this phenomenon and to introduce the disturbing effects due to the soft tissues.

PsycINFO classification: 4140

Keywords: Upper limb; Robotic model; 3D kinematics; External markers

1. Introduction

Several optoelectronic systems are now able to describe, with good accuracy, the trajectories of emittive or reflective markers in the laboratory frame. Application software was specifically developed for gait analysis. Markers are put on the skin of each body segment from which stick diagrams are drawn to roughly represent the body in motion. Stick diagrams may be considered as a simplified model of the moving limb (Youm and Yih, 1987). It is assumed that body segments are solids connected by articular groups or joints to which the laws of solid kinematics can be applied (Cappozzo, 1984). This is why at least 3 markers are fixed to each segment allowing a 3-dimensional study.

In the biomechanic field, the geometrical figure drawn by the 3 markers fixed on a same segment is not undeformable throughout the movement. This is due to both inaccuracies of the optoelectronic system and far more elastic deformation of skin-fixed markers. It is not reasonable to directly apply the laws of solid kinematics upon the trajectories of segmental markers. Woltring et al. (1985) defined a segmental frame and used a least-square technique to best fit the instant location of the segmental frame to the instant position of each marker of the segment. The 3 best markers among all markers fixed upon each segment were developed by Chèze et al. (1995). With this technique, the angular deformations between the sides of the triangle defined by the 3 markers are optimized throughout the motion. A mean shape of the best triangle is calculated. This solidified triangle is best fitted to each position of the real marker triangle using a least-square technique.

The apices of the solidified triangle are fitted to those of the instant one and the individual markers replaced. Any further computation uses the coordinates of the apices of the solidified triangle. The laws of solid kinematics can then be applied to these modified trajectories of solidified markers.

In kinematics, we treat continuous trajectories of points, whereas only discrete locations of markers are available from a video analysis system. Kinematics are generally approximated by substituting finite small displace-

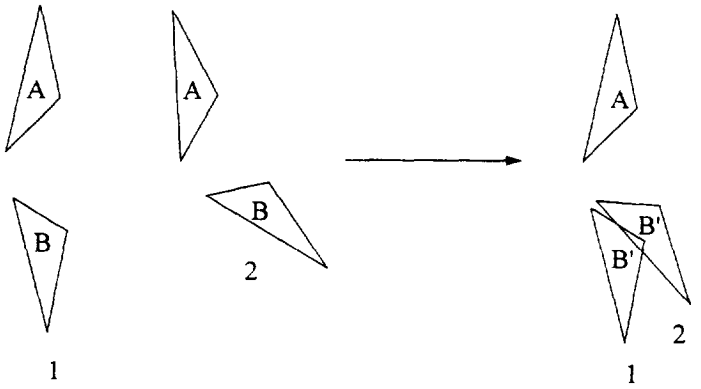

Fig. 1. The location of real markers and the situation allowing the calculation of kinematic components.

ments to instantaneous velocities corresponding to the relative displacement of the segmental triangle B versus the segmental triangle A computed between two successive instants of time 1 and 2 (Fig. 1).

The parameters describing the finite screw displacement are: location and orientation in space of the screw axis, the angle and translation along it. Another way to describe the relative displacement between the two adjacent segments is to use a sequence of 3 successive rotations (Grood and Suntay, 1983). These rotations must have an anatomic significance for clinical applications. In this case, a mechanism analogous to the joint is defined to model the variations of the anatomic angles and the scattering of the joint center. Robotics may provide an answer to this modeling difficulty.

An elementary link is associated with each degree of freedom (df) in rotation (flexion, abduction, axial rotation). The size of each elementary link is calculated through an inverse process from the matrix form describing the location of frame B with respect to frame A. The determination of the analogous mechanism to the articular group gives the direction of the elementary axes of rotation (flexion, abduction, axial rotation) known in local frames A and B. This is obtained from preliminary testings. The subject, instrumented with skir markers, is asked to move each of his joints with simple movements: pure flexion and axial rotation, and circumductions of different magnitudes.

Each articular group is modeled as a mechanism where each df is represented by a separate joint. The analogous mechanism of the entire upper limb is obtained by assembling the different articular groups connected together by

longitudinal links. The mechanical structure of the upper limb is then animated: the changes in the joint variables over time are computed using an inverse process from the trajectories of segmental markers. Often the result obtained are not compatible with the anatomical reality. The elbow shows variations in abduction component which cannot be neglected. This can be explained in part by the movement of the analogous mechanism to that of the articular group defined from the displacement of frames affixed to external triangles *A* and *B*. These triangles move themselves with respect to internal bones. The laws of displacement of the internal structure are different to those obtained from external marker treatment. To address this problem, it is necessary to have an idea about the kinematic behavior of the anatomic structure. This is obtained from tests carried out on specimens. It is then assumed that the joint constraint equations obtained from the specimen can be applied to the movements of the internal structure of a living subject.

The existence of constraint between the articular variables allows us to introduce new df. They correspond to the perturbed movement due to external markers and skin movement with respect to the underlying bone. The modified mechanical structure takes into account the articular constraints and the perturbing effect of the soft tissues in relation to the bone. The changes in the df of the new structure are computed whilst carrying out a task. It is difficult to directly validate the simplifying hypotheses used to represent the relative displacement of external markers with respect to internal bones. Markers, close to bony landmarks, indirectly confirm the retained assumptions. The methodology used for upper limb may be extended, after specific testings, to the motion of the lower limbs during gait.

2. From the individual marker trajectories to the relative displacement of segments

2.1. Solidification procedure

Video-based motion analysis systems are commonly used to study joint kinematics. This is often accomplished by recording the movement of 3 or more individual markers put over the skin of each moving segment (Cappozzo, 1984; Kadaba et al., 1990). If the marker representation of the body segment maintained a rigid shape throughout the motion, rigid body theory could be directly applied to describe the marker trajectories. However, a rigid shape is not

maintained, primarily because of skin and soft tissue movements caused by displacements as large as 2 cm between a marker and its corresponding anatomical landmark (Andriacchi, 1987). Consequently, rigid body theory becomes less accurate for performing kinematic calculations based on the measured marker coordinates.

Both a physical and a numerical solution can be proposed to address this problem. The physical solution involves mounting 3 markers on a rigid device often strapped over a moving muscle mass rather than over an anatomical landmark with little intervening soft tissue (Stokes et al., 1989). As a result, soft tissue introduces motion perturbations which increase with the marker to bone distance. Furthermore, such perturbations are difficult to remove by a low-pass filter since their frequency content is close to that of the motion.

The numerical solution proposed by Chèze (1993) involves a least-square procedure to transform measured data from individual markers into a rigid body. Individual markers can be mounted over anatomical landmarks, minimizing soft tissue perturbations. The solidification procedure is composed of 3 consecutive steps. All steps utilize the directions given by any two markers rather than the positions of the markers, as Dimnet (1978) has shown that the directions are more accurate. First, the 3 markers which define the least-perturbed triangle are identified over the entire motion Then the shape best fitting this time-varying triangle is computed. Third, the position of the 'solid' best-fit triangle is calculated at each point of the motion. Afterwards, the 3 measured marker coordinates are replaced by those estimated by the best-fit triangle. It has to be noticed that the solidification procedure is efficient to correct the measurement errors due to skin elasticity, which deforms the marker triangle, but is unable to correct a global shift of the whole triangle with respect to the underlying bone.

To validate this method, a sensitivity analysis was performed on experimental data taken during the swing phase of gait. A 25% reduction in the kinematic errors was obtained when the maximum distance between body markers was small (< 15 cm).

2.2. Numerical treatment of external intersegmental displacements

The parameters of finite screw displacements are presented in Fig. 2. Let R_0 be the fixed frame and S a moving solid. The frame R is fixed to S. At the instants of time t_1 and t_2, R is in the positions R_1 and R_2, respectively. A screw axis Δ is defined passing through I and of unit vector $\underline{k}$. It is possible to

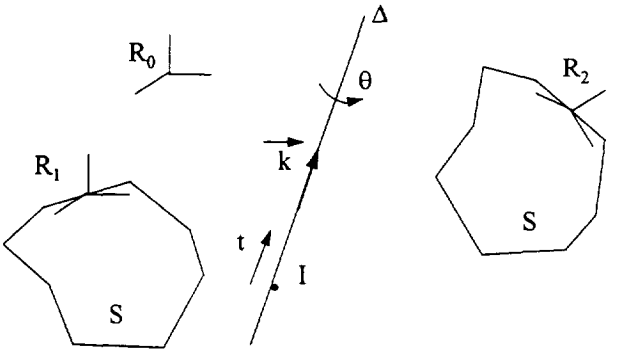

Fig. 2. The screw displacement moving the solid S from position 1 to position 2.

move S from R_1 to R_2 using both a translation t and a rotation θ around Δ. $\bar{k}$ and θ are obtained through a mathematical treatment from the rotation matrix $\underset{\sim}{{}^{1}_{2}R}$:

$\underset{\sim}{{}^{1}_{2}R} = \cos(\theta)[I] + \tilde{k}\sin(\theta) + k.k^{t}(1 - \cos(\theta))$ with

$$k = \begin{bmatrix} kx \\ ky \\ kz \end{bmatrix} \quad k^{t} = [kx\ ky\ kz] \quad \tilde{k} = \begin{bmatrix} 0 & -kz & ky \\ kz & 0 & -kx \\ -ky & kx & 0 \end{bmatrix}$$

θ and t are obtained using the following formulae:

$$\begin{cases} \theta = \cos^{-1}\left[\left(\text{Trace}\left({}^{1}_{2}R\right) - 1\right)/2\right] \\ t = O1O2'.k \end{cases}$$

The concept of screw displacement may be adapted to the biomechanical situation. Let two triangles A_1 and B_1 representing two adjacent body segments at instant t_1 (Fig. 1). They are located, respectively, in A_2 and B_2 at instant t_2. The kinematical approach considers the relative displacement $B_1'B_2'$ of triangle B with respect to A assumed to be fixed between instant t_1 and t_2. The triangle apices correspond to skin fixed markers not very accurately known in space. Position B_2' is often very closed to position B_1', so that the matrix form $\underset{\sim}{{}^{1}_{2}R}$ is very perturbated. The calculation of the vector $\bar{k}$ components is altered by large errors. Chèze analyzed this phenomenon and its corresponding consequences. An alternative approach has been proposed. It consists in computing the screw parameters with respect to a relative displacement between two distinct positions B_i and B_j. If the measured displacement is quite significant compared to the

uncertainties on the marker locations, then the finite displacement parameters can be obtained with good accuracy.

3. The mechanical structure of the articular group connecting two body segments

3.1. Introduction

Modeling the mechanism relative displacement of segment B versus segment A implies that the functional axes and the centers are known. Here, each of the body segment is materialized by the solidified triangle of the skin-fixed markers. Previous studies attempted to directly locate the internal bony structure with respect to the triangle of external markers (Gignoux, 1994) where the shape of the bones was obtained from a data bank. These shapes were roughly adapted to subject's size, but the bony morphology was not taken into account. Moreover, the functional axes and the centers were defined from the shape of bone assuming that they were corresponded with anatomical directions. This last assumption was not accurate and resulted in a lack of reproductivity. Another approach has been tested to directly determine the functional parameters (axes and centers) with respect to the external triangles without the above assumption relative to the shape of internal bones.

3.2. Functional parameters in moving upper limbs

These functional parameters are the axes and the centers of rotation. They are determined from a simple pretest. The subject is instrumented with the same markers in the same positions as used in the main testing. These pretests are performed on one articular group only. Only one df is studied for the axis determination while several df are simultaneously moved to locate the joint center.

3.2.1. Axes of rotation

An experimental protocol has been defined to isolate an elementary rotation for each articular group (shoulder, elbow and wrist joints) using video cameras. Tests that are as close as possible to pure flexion (or axial rotation) are retained. Subjects are asked to move their articular group, to obtain a pure movement of flexion. The angular velocity must be low in order to avoid perturbing displacements of smooth masses. Several experimental devices have been used to obtain

the pure movement corresponding to the selected df and to avoid coupling effects with the others movements. The best data were obtained teaching the task to the subject with successive feedbacks after result analysis.

Two kinds of numerical treatment have been selected. A global kinematic treatment defines for each instant of time i the global relative screw axis moving the solidified triangle of the segment between two sufficiently distinct positions B_i and B_j. For the entire movement, a bundle of screw axes is obtained. If the bundle is not too scattered, it can be claimed that the pure motion was correct. The mean axis of the bundle is considered as the functional axis of the pure movement of flexion (or rotation). It is then located in each external frame affixed to triangles A and B.

A global geometric approach has also been tested. The apices of triangle B describing relative trajectories with respect to the segment A are assumed to be fixed. Each marker movement is comparable to a rotation about a fixed axis, then the trajectories are roughly planed and look like circles. A mean plane best fitting the 3-dimensional trajectories is calculated afterwards. It is then possible to determine if each trajectory is either best fitted to a single mean plane or to several. The trajectories are projected onto the mean plane and corresponding projections are fitted to a circle. The axis of the circle perpendicular to the mean plane and passing through the circle center is assumed to be the axis of the pure rotation. In the case of several mean planes, the corresponding axes are calculated and the global motion is decomposed in several phases.

3.2.2. Centers of rotation

This following analysis deals with both the wrist and the shoulder. In the pretests, markers have the same location as used in the main experiment. The difference lies in the kind of movement. The upper limb is fixed with the exception of the studied articular groups. The subject moves his articular group with a circumduction movement. Several angular motions describe a cone. The method used to define the position of the joint center follows.

The articular groups are idealized as ball and socket joints. Let A and B be the triangles representing the adjacent body segments. The relative movement of B with respect to A is a rotation about an unknown point. The principle consists in finding a line Δ belonging to B with respect to a point belonging to A which is minimum throughout the total movement. An initial position is chosen for Δ. It corresponds to the estimated direction Δ_0 of the longitudinal axis of the body segment B. An initial position A_0 is chosen for the joint center C: it is the estimated location of the center of rotation in the segment A. During motion, Δ_0 moves with respect to (w.r.t.) A. Let Δ_{0i} be its position at the instant i. A_0 is

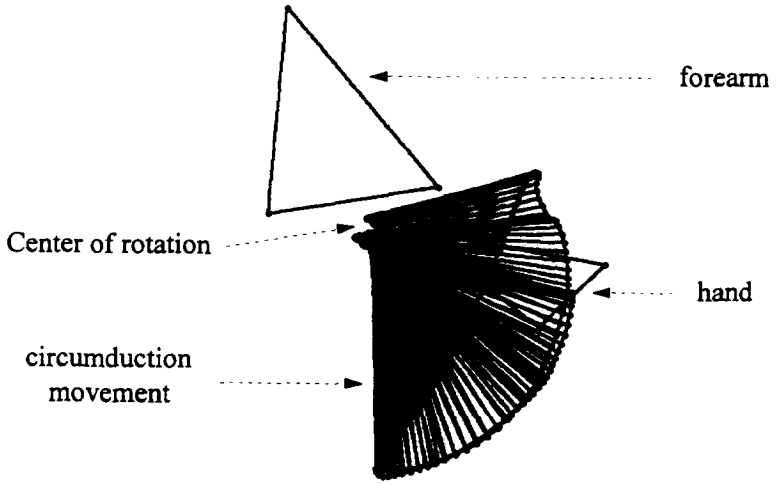

Fig. 3. The circumduction movement of the wrist joint.

then orthogonally projected upon Δ_{0i}: let H_{0i} be this projection. The cluster of points H_{0i} in the frame A has a barycenter: let A_1 be this point. At each instant i, A_1 coincides with a point named B_{1i} belonging to B. The cluster of points B_{1i} has a barycenter B'_1. In frame B, the direction Δ_0 is altered in Δ_1 so that it passes through B'_1. The process continues, Δ_1 and A_1 replacing Δ_0 and A_0, respectively, until the distance between the cluster barycenters is stabilized at a minimum value. The final location A_n is assumed to be the center of rotation in frame A. Δ_n is the longitudinal axis of the segment B. The changes in the normal distances between the center A_n and the instant locations of longitudinal axis Δ_n of B give the linear offset of the joint during motion.

Fig. 3 shows the results obtained for the wrist, which has a single center of rotation. In the case of the shoulder, a circumduction movement of large angular magnitude displays an important scattering of the articular center. The shoulder must be considered as an articular group with 2 centers: one deals with a circumduction movement of small angular magnitude, the arm being roughly vertical (Fig. 4). It has been verified that this rotation center corresponds to the anatomic center of the humerus head. The second center corresponds to a circumduction of small magnitude when the arm is roughly horizontal (Fig. 5).

Fig. 6 illustrates the functional parameters of the upper limb when articular groups are combined. From the circumduction movements of the longitudinal axes of hand, the centers of the wrist and shoulder and the corresponding linear

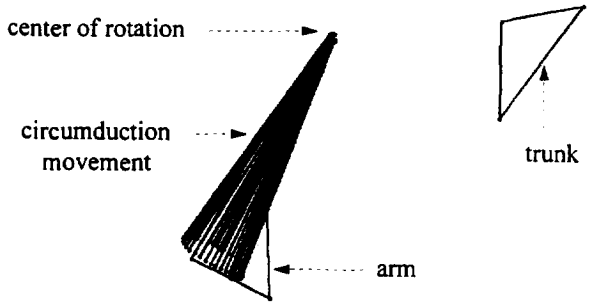

Fig. 4. The circumduction movement of the shoulder joint, the arm being roughly vertical.

articular offsets are estimated. The single rotation movements give: flexion axes of shoulder, elbow and wrist, axial rotation axes of the arm and of the forearm.

The internal structure of the analogous robot of the moving upper limb is defined from the functional parameters known from these pretests.

3.3. Identification of the robot structure

It is assumed that longitudinal links of the mechanism representing the arm, forearm and hand coincide with the longitudinal functional axes defined from pretests. The external segmental triangles representing the arm, forearm and hand are assumed to be rigidly connected to corresponding longitudinal links of the mechanism. Each articular group connecting two successive longitudinal links of the mechanism is assumed to have 3 angular df.

The technique of Denavit and Hartenberg is based upon an initial postulate: a mechanism must be considered as a chain of segments connected by joints with

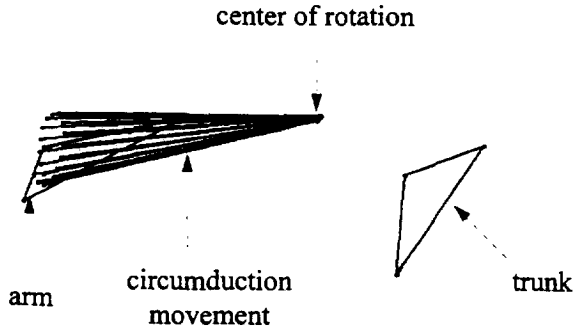

Fig. 5. The circumduction movement of the shoulder joint, the arm being roughly horizontal.

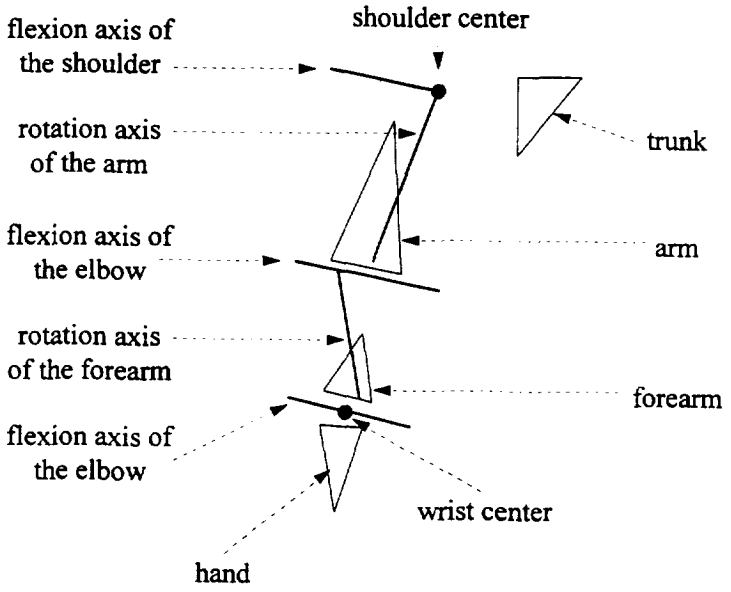

Fig. 6. The result of assembling the functional parameters of the upper arm.

a single df (Fig. 7). The geometry of each link S_i is described: the angular offset α_i between down and up joint axes Z_{i-1} and Z_i, and the linear offset a_i between them.

The location of each link S_i with respect to previous one S_{i-1} is defined: one

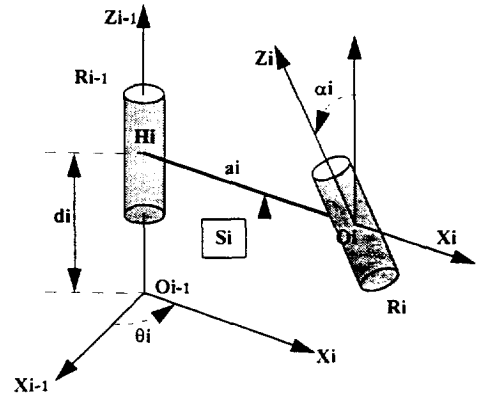

Fig. 7. The Denavit–Hartenberg parameters locating a solid S_i w.r.t. a solid S_{i-1}.

translation d_i along Z_{i-1} and one rotation θ_i around Z_{i-1}, where d_i is constant while θ_i is variable.

A matrix form is associated to each link S_i and is a function of the geometric parameters a_i and α_i and on the parameters θ_i and d_i defining the position of the link S_i versus S_{i-1}.

The frame F_{i-1} $(O_{i-1}, X_{i-1}, Y_{i-1}, Z_{i-1})$ is affixed to the solid S_{i-1}. The frame F_i (O_i, X_i, Y_i, Z_i) is affixed to the solid S_i. The matrix form $\underline{{}_i^{i-1}T}$ locates the frame F_i w.r.t. F_{i-1}. It is obtained through the following formula.

$$\underline{{}_i^{i-1}T} = \begin{bmatrix} C\theta_i & -S\theta_i & 0 & 0 \\ S\theta_i & C\theta_i & 0 & 0 \\ 0 & 0 & 1 & d_i \\ 0 & 0 & 0 & 1 \end{bmatrix} \begin{bmatrix} 1 & 0 & 0 & a_i \\ 0 & C\alpha_i & -S\alpha_i & 0 \\ 0 & S\alpha_i & C\alpha_i & 0 \\ 0 & 0 & 0 & 1 \end{bmatrix}$$

This matrix form allows to transfer the coordinates of any point M belonging to S_i in the frame affixed to S_{i-1}:

$$\underline{O_{i-1}M^{i-1}} = \underline{{}_i^{i-1}T}.\underline{O_iM^i}$$

where $\underline{O_iM^i}$ represents the coordinates of M in frame S_i, $\underline{O_{i-1}M^{i-1}}$ the coordinates of M in frame S_{i-1}. This formula, applied to all links constituting the robot, is used to compute the coordinates of any point of the robot structure in any fixed or moving frame.

3.4. Identification of the model of an articular group using the Denavit-Hartenberg formalism

For each articular group, the problem may be stated as: a solidified down triangle A is rigidly connected to the longitudinal axis Δ_A of the low segment.

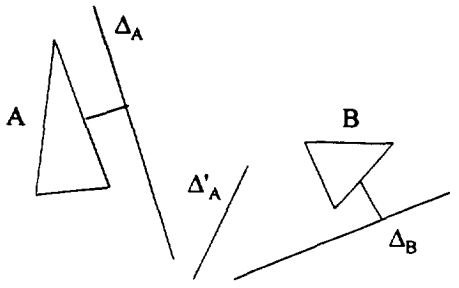

Fig. 8. Experimental results before joint modeling.

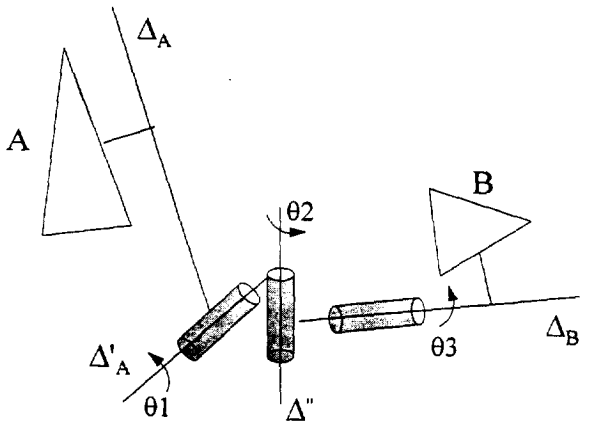

Fig. 9. The principle of joint modeling.

In the same conditions, the solidified up triangle B is rigidly fixed to the up axis Δ_B. Pretests have determined a flexion axis Δ'_A of known position w.r.t. the low segment A (Fig. 8).

The relative position of B w.r.t. A is based on 6 articular variables: 3 rotations and 3 translations. The identification of the articular group model is obtained using 3 links of Denavit–Hartenberg connected in a chain, rotation axes coinciding with functional axes. The first rotation is a flexion about Δ'_A axis. The third rotation (axial rotation) corresponds to Δ_B axis while the second rotation deals with an abduction rotation around Δ'', this axis being perpendicular to both axes Δ'_A and Δ_B (Fig. 9).

The analogous mechanism to the articular group connecting A to B is compound of 4 links:

- S_A,
- S_1 rotates versus A of an angle θ_1 around Δ'_A,
- S_2 rotates versus S_1 of an angle θ_2 around Δ'',
- S_B rotates versus S_2 of angle θ_3 around Δ_B.

The matrix form $\overset{A}{\underset{B}{T}}$ is known at each instant of time from the locations of triangles A and B. The Denavit–Hartenberg formalism is used to express the matrix form $\overset{A}{\underset{B}{T}}$ as a function of the 3 angular variables θ_1, θ_2, θ_3 and 3 of the linear geometric parameters of internal links: a_1, d_2, a_3. They allow the instant value of the offset between rotation axes Δ'_A and Δ_B to be described.

An inversion procedure allows the instant value of the 6 parameters to be calculated characterizing the articular group (θ_1, θ_2, θ_3, a_1, d_2, a_3) from the

numerical values of the matrix form ${}^{A}_{B}T$. But the Denavit–Hartenberg convention implies that the value $a_1\ d_2\ a_3$ describing the geometry of links would be constant throughout the movement. Mean sizes of links $\overline{a1}\ \overline{d2}\ \overline{a3}$ are calculated from instant values $a_1\ d_2\ a_3$ and then introduced in the new matrix form ${}^{A}_{B}T$. This operation does not modify the instant values of θ_1, θ_2, θ_3 because the rotation matrix ${}^{A}_{B}R$ calculated remains the same. Replacing $a_1\ d_2\ a_3$ by $\overline{a1}\ \overline{d2}\ \overline{a3}$ in the matrix form ${}^{A}_{B}T$ modifies very slightly the offset between rotation axes Δ'_A and Δ_B. These changes can be neglected. Thus, 3 angular values θ_1, θ_2, θ_3 are enough to correctly model any articular group. Angular displacements and linear offsets are taken into account by only 3 df and a well-adapted geometry of links. Assembling 3 articular groups gives a mechanism with 9 df. Its geometric structure is known directly from the pretests (longitudinal links) and indirectly from numerical treatment of each articular group (intra-articular links).

4. Accounting the effects of fat and muscles

The analogous mechanism of the moving upper limb has 9 df. Each articular group is modeled sequentially by 3 rotations: flexion, abduction, axial rotation. Results obtained for flexion angles are very satisfying. But other values do not totally relate with anatomic observations. It is necessary to define anatomic constraints, compatible with the functioning of internal joints, and then to modify the structure of the mechanism so as to both respect the anatomic constraints and to take into account the perturbing effect of smooth masses between external markers and internal bones.

In anatomy, coupling effects are observed, so mathematical relations may connect two articular variables. These constraint relations decrease the degree of mobility of the corresponding group. In the case of the elbow, anatomists claim that there is no abduction during any movement and that the wrist has no axial rotation. Corresponding constraints would be $\theta_2 = 0$ (elbow) and $\theta_3 = 0$ (wrist). It was necessary to experimentally validate these anatomic observations.

A upper limb specimen has been prepared, all muscles being removed, but articular materials have been entirely kept. Reflective markers were fixed in the same position as in the living subjects. The same movements as those performed in pre-experiments were realized and numerically treated. The results are given below.

(1) The axes of single rotation (flexion axes and pronosupination axis) are more stable than those found in living subjects. The joint centers are localized in

a very small area. The location of functional axes and centers corresponds to those of the specimen.

(2) The structure of the specimen have been modeled in the same conditions as in the living subject (mechanism with 3 df for each of the 3 articular group). The value found for the abduction θ_2 of the elbow is close to zero ($\theta_2 = 0 \pm 1°$). For the wrist, the axial rotation is also very small ($\theta_3 = 0 \pm 1°$).

An indirect validation was also carried out in the living subject. External markers are placed near bony structures as close as possible to flexion axes of elbow and wrist. Markers fixed on the internal side of the upper limb are poorly visible on living subjects. Specific experiments have been defined with numerous cameras, different camera locations in a great number of tests. In these conditions, the new matrix forms ${}^{A}_{B}\underline{T}$ describing the function of each articular group are obtained. The corresponding model with 3 df in rotation for each joint was applied. The corresponding values for elbow abduction and wrist axial rotation were $\theta_2 = 0 \pm 2°$ and $\theta_3 = 0 \pm 1.5°$, respectively.

4.1. New model of the upper limb

In the new model of the upper limb, the following hypotheses are assumed.

(1) The internal structures in a living subject respects the same anatomic constraints as those observed in a specimen without any fat and muscle. This has been verified on living persons under specific conditions allowing the effects of smooth masses to be neglected.

(2) The use of constraint relations decreases the number of degrees of mobility of the mechanism. It allows the introduction of new degrees of mobility in each articular group concerned by a constraint relation (elbow and wrist). These new degrees of mobility were chosen to represent the perturbing effect of the smooth masses interposed between external markers and internal bone. To solve the numerical problem, another hypothesis has been necessary.

(3) It is assumed that at the level of the hand, the smooth masses effect is negligible (no fat and no muscles between markers and internal bones). To reinforce this hypothesis, a small wooden board has been solidly fixed to the hand and 3 markers glued upon this device.

At the wrist, axial rotation, existing in the initial model, is suppressed to respect the anatomic constraint $\theta_3 = 0$. The modified model introduces:

- an axial rotation θ'_0 around the longitudinal axis Δ_A. θ'_0 represents the perturbing effect of smooth masses between skin and forearm a flexion rotation θ'_1 around the flexion axis Δ'_A,
- an abduction rotation θ'_2 around the abduction axis Δ''.

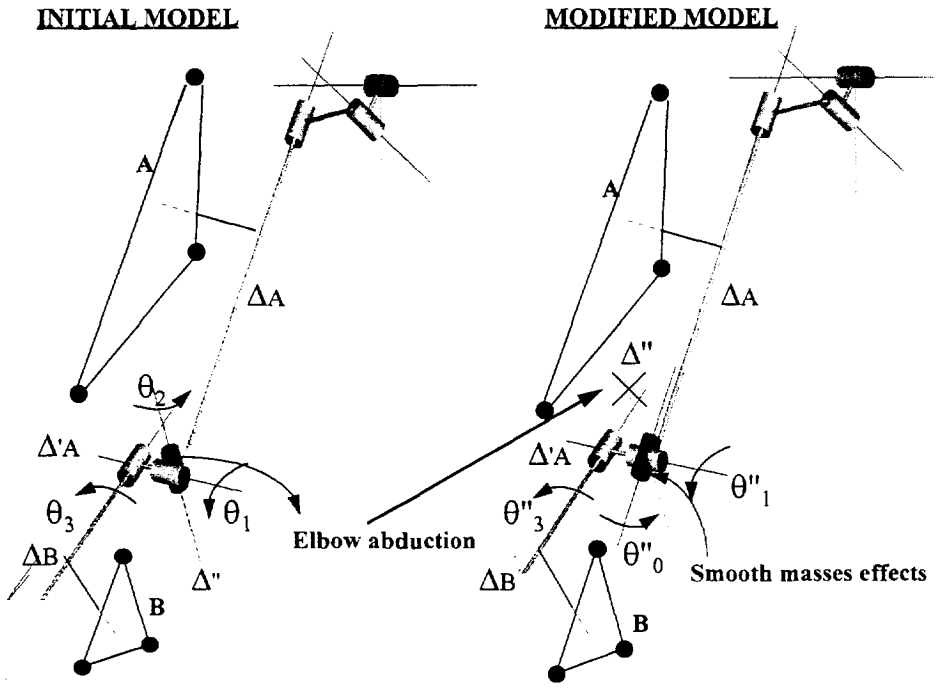

Fig. 10. The elbow joint (A, arm; B, forearm) before and after modification taking the anatomic specificities into account.

The angular relative position of the up segment B with respect to the down segment A is numerically defined from the rotation matrix form ${}^{A}_{B}R$. Initially the inverse procedure gave 3 angles (θ_1, θ_2, θ_3: flexion, abduction, axial rotation), with the modified model the inverse procedure applied to the same matrix form gives θ'_0, θ'_1, θ'_2 (smooth masses rotation, flexion and abduction, axial rotation being null).

The new model has been directly validated using specimen and indirectly with subjects instrumented with numerous markers and more particularly with marker locations coinciding with functional axes. The results allow smooth masses perturbing effects in some tasks of the current life to be evaluated.

The triangle A in Fig. 10 of the wrist is now the triangle B of the elbow. In the initial model, the rotation matrix of the elbow ${}^{A}_{B}R$ was decomposed in a sequence of 3 successive rotations: flexion θ_1 around Δ'_A, abduction θ_2 around Δ'' and axial rotation (pronosupination) around Δ_B. In the modified model, the same matrix form ${}^{A}_{B}R$ is decomposed as:

- an axial rotation θ''_0 around the longitudinal axis Δ_A of arm (this rotation θ''_0 represents the smooth masses effects between skin and arm),
- a flexion rotation θ''_1 around Δ'_A,
- an axial rotation θ''_3 around Δ_B. This last angle θ''_3 is the resultant of the smooth masses effects θ'_0 between skin and bones at the level of the forearm and the pronosupination angle $\theta''_3-\theta'_0$,
- the abduction is assumed to be null (respecting the anatomic constraint).

Anatomic studies with specimen did not give any constraint relation between articular variables of the shoulder. In the initial model, the rotation matrix $\overset{A}{\underset{B}{R}}$ between the segment of the arm B and the segment of the torso A gave: flexion θ_1, abduction θ_2 and axial rotation θ_3 through an inverse procedure. The axial rotation θ_3 is the sum of the smooth masses angle θ''_0 and the internal rotation of the arm $\theta_3-\theta''_0$. The global model of the articular group corresponding to the shoulder is represented by the matrix form $\overset{A}{\underset{B}{T}}$ where A corresponds to the torso and B to the arm. The rotation matrix $\overset{A}{\underset{B}{R}}$ (a part of $\overset{A}{\underset{B}{T}}$) gives the angular variables θ_1 θ_2 θ_3. The instant values of offset a_1 d_2 a_3 are obtained at the instant value of $\overset{A}{\underset{B}{T}}$. So a_1 d_2 a_3 must be considered as linear variables, but this is not compatible with the initial postulate: each articular group is modeled by 3 revolute joints connected by links with a constant geometry. The linear offset may be modeled by constants $\overline{a1}\,\overline{d2}\,\overline{a3}$ which correspond to the mean of instant values a_1 d_2 a_3.

A new value of $\overset{A}{\underset{B}{T}}{}^*$ may be obtained from instant value of θ_1 θ_2 θ_3 and from $\overline{a1}\,\overline{d2}\,\overline{a3}$ by replacing a_1 d_2 a_3, respectively. Applied to the real location of B, $\overset{A}{\underset{B}{T}}{}^*$ gives a new location for the triangle A^* which is slightly different from the real torso triangle A. A 3-dimensional translation moves A^* to A. It can be proposed that the shoulder articular group is modeled by a mechanism having 3 revolute joints (θ_1 θ_2 θ_3) and constant offsets $\overline{a1}\,\overline{d2}\,\overline{a3}$.

4.2. Smooth masses effects

Each articular group is numerically defined by a matrix form $\overset{A}{\underset{B}{T}}$ connecting the frame A to the frame B. This matrix, incorporating rotation and translation, must be described by 6 parameters (3 rotations and 3 translations). The mechanism representing this articular group is modeled on 3 revolute joints (variables θ_1 θ_2 θ_3) and 3 prismatic joints (variables a_1 d_2 a_3). To limit the number of degrees of freedom, it was decided to keep the 3 revolute joints and to lock the prismatic ones in their mean value $\overline{d5}, \overline{d6}, \overline{a6}$. The lack of information due to the simplified model is very low in wrist and elbow. It is not strictly

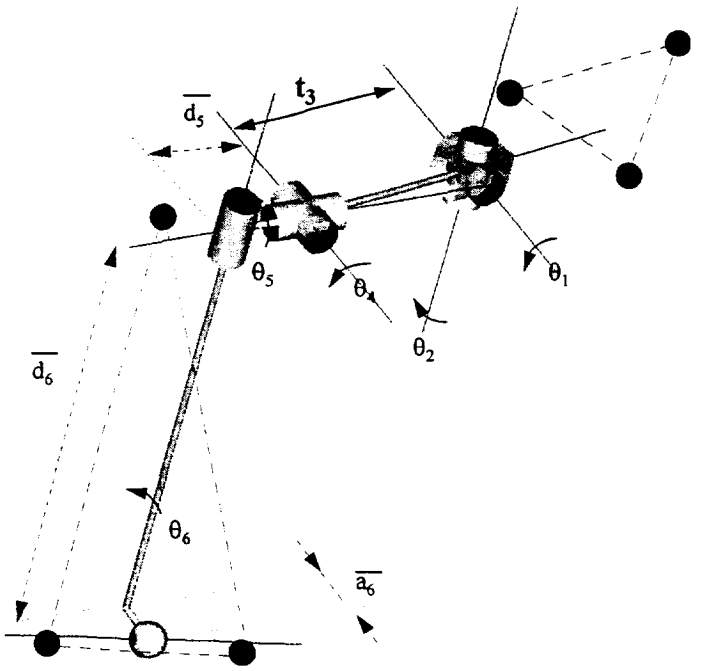

Fig. 11. The new model of the shoulder joint representing the effects of scapula and clavicula.

negligible in the case of the shoulder. This is why a new model of the shoulder complex has been tested. It is much more adapted to the anatomic observation. Pretests on living subjects clearly show the existence of two separate clusters of joint centers. The first deals with movements of small magnitude when only the scapulohumeral joint is solicited. The second is observed when the arm is moved around a horizontal position. It corresponds to the motion of a set of bones: humerus, scapula and clavicula. It is possible to represent this anatomic reality by a model with 6 df (5 rotations and one translation) (Fig. 11):

- 2 intersecting rotations θ_1 θ_2 represent the down center,
- 3 intersecting rotations θ_4 θ_5 θ_6 represent the up center (spherical joint),
- 1 translation t_3 represents the offset between the two centers.

The mechanism is roughly comparable to the anatomic reality. A first longitudinal link S_4 correspond to the set clavicula/scapula moving with respect to the torso A. The arm B is connected to the scapula by mean of scapulo-humeral joint assumed to be a spherical joint. This last model gives good results which correspond to clinical observations.

5. Discussion and conclusion

A robotic model of the moving upper limb has been presented. The experimental study is based upon 3 markers fixed on each moving segment. The triangle drawn by the segmental markers is solidified and an external frame is affixed to it. The relative position in space of successive segmental triangles is then calculated. It allows the instant configuration of the articular complex connecting the two adjacent segments to be defined. This configuration must be expressed in terms of anatomic rotations if clinical applications are wanted based on new experimental pretests. They allow axes and centers of rotation versus external frames to be directly located without X-ray examination.

The model of each articular group might have 6 df: 3 rotations for 3-dimensional angular displacements and 3 translations to take into account the scattering of rotation centers. For simplification purposes, each articular group is modeled using only 3 angles, the offset of the joint centers being represented by the 3 angles and by the geometry of the 3 elementary links connected together. The initial global model of the upper limb shows 9 df. Each local model representing each articular group is modified so as to introduce the effect of fat and muscles interposed between external markers and internal bones. Each model of the effects of smooth masses is based upon experimental tests on an anatomic specimen. They confirmed the existence of anatomic constraints between the variables. In the upper limb, the expression of the law of constraint is relatively simple. Anatomic variables are close to zero during any motion of the upper limb (elbow abduction and wrist axial rotation), which introduces two constraints among 9 df describing the external structure. This means that the internal structure has only 7 real degrees of mobility. The difference in degrees of mobility between external (9) and internal (7) is used to introduce 2 degrees of mobility to represent the effects of smooth masses interposed between markers and bone. These hypotheses have been tested and the smooth masses effects have been modeled.

In the location of axes and centers w.r.t. external frames, a slight change in the direction of rotation axes greatly affects the distribution of angle values during the motion. Reproducible results are obtained through very strict observance of the protocol. The perturbing effect induced by the smooth masses can vary as a function of the task. When the upper limb is pointing to an object, the retained perturbing effects of smooth masses at the level of forearm and arm are axial rotations.

Between an external frame defined from superficial markers and the corresponding internal bone, six df might be used to describe 3-dimensional displace-

ments. Measurement inaccuracies are such that a more sophisticated model would be inoperative. In this context, the main displacement is represented and a coefficient is created: it allows the lost information to be quantified. In the case of an upper limb pointing to an object, the main displacement of arm and forearm external frames versus internal bones are found to be rotations around longitudinal axes. A living subject instrumented with markers has been submitted to a 3-dimensional X-ray analysis in the two external positions in the movement. From the 3-dimensional images of both bones and markers, global displacements of markers, with respect to underlying bones, have been computed and confirm the hypothesis.

The upper limb has more degrees of freedom than necessary to realize a given task in 3-dimensional space. The internal simplified structure, without participation of the hand and back, has 7 df. In which way does the neuromuscular system control this redundancy? In order to understand this phenomenon, it has appeared necessary to define a good model representing the moving structure of an upper limb so as to describe the laws of variations of each of articular parameter task.

References

Andriacchi, T.P., 1987. Clinical applications of the SELSPOT system. Biomechanics Symposium ASME 84, 339–342.

Cappozzo, A., 1984. Gait analysis methodology. Human Movement Sciences 3, 27–50.

Chèze, L., 1993. Contribution à l'étude cinématique et dynamique in vivo de structures osseuses humaines par l'exploitation de données externes, Thèse no. 89–93, Université Claude Bernard, Lyon.

Chèze, L., B.J. Fregly and J. Dimnet, 1995. A solidification procedure to facilitate kinematic analyses based on video system data. Journal of Biomechanics 28, 879–884.

Dimnet, J., 1978. Contribution à l'étude biomécanique des articulations par l'utilisation des procédés radiographiques. Thèse d'Etat no. 7823, Université Claude Bernard, Lyon.

Gignoux, P., 1994. Etude tridimensionnelle des sollicitations mécaniques d'une hanche en mouvement. Thèse no. 23–94, Université Claude Bernard, Lyon.

Grood, E.S. and W.J. Suntay, 1983. A joint coordinate system for the clinical description of three-dimensional motions: applications to the knee. Journal of Biomechanical Engineering 105, 136–144.

Kadaba, M.P., K.K. Ramakrishnan and M.E. Wootten (1990) Measurement of lower extremity kinematics during level walking. Journal of Orthopaedic Research 8, 383–392.

Stokes, V.P., C. Andersson and H. Forssberg, 1989. Rotational and translational movement features of the pelvis and thorax during adult human locomotion. Journal of Biomechanics 22, 43–50.

Woltring, H.L., R. Huiskes and A. de Lange, 1985. Finite centroïd and helical axis estimation from noisy landmark measurements in the study of human kinematics. Journal of Biomechanics 18, 379–389.

Youm, Y. and T. Yih, 1987. Kinematic simulations of normal and abnormal gaits. Biomechanics of Normal and Prosthetic Gait 4, 23–29.